EFFECTS OF CARBON NANOFIBER Z-THREADS ON THE LONGITUDINAL COMPRESSIVE STRENGTH OF UNIDIRECTIONAL CFRP LAMINATES

Sebastian Kirmse[1,2], Keonhyeong Kim[3], Bikash Ranabhat[1,2], Kuang-Ting Hsiao[3,*]

University of South Alabama
Mobile, Alabama 36688, United States

[1]College of Engineering
[2]Systems Engineering Program
[3]Department of Mechanical Engineering
*Corresponding Author: Email: kthsiao@southalabama.edu; Phone: +1 (251) 460-7889

1. ABSTRACT

In this study, unidirectional carbon fiber prepregs that contain long carbon nanofiber (CNF) z-threads as a through-thickness (z-directional) reinforcement were manufactured. The CNF z-threads are long enough to thread through multiple carbon fiber (CF) arrays, which creates a multi-scale CNF/CF/resin-composite. The CNF z-threaded prepregs were manufactured using an electric-field aligned flow-transferring process. It was hypothesized that the CNF z-threads with the zig-zag threading pattern reinforces the interlaminar and intralaminar regions of the CFRP laminate thus improve the compressive strength by reducing the chance of carbon fiber buckling. Compressive testing was performed per modified version of ASTM D695 (i.e., SACMA SRM 1R-94) to evaluate the compressive strength of the CNF z-threaded CFRP (ZT-CFRP) laminates. The samples were manufactured using AS4 carbon fibers, EPON 862/Epikure-W resin and a 1wt% CNF content. ZT-CFRP testing results were compared with unaligned CNF-modified CFRP (UA-CFRP) and unmodified CFRP samples to investigate the impact of the CNF z-threads on the compressive strength. Results showed an increase of ~15% for the compressive strength of ZT-CFRPs, whereas the UA-CFRPs experienced a decrease of ~8% when compared to unmodified CFRPs. It was concluded that CNF/carbon fiber interlocking stops and delays crack growth, and helps to stabilize carbon fibers from further buckling.

2. INTRODUCTION

Carbon fiber reinforced polymer (CFRP) laminates are widely used in many applications since they are strong and lightweight. However, due to the multi-ply configuration, traditional CFRP laminates are vulnerable to matrix-sensitive damages, e.g., compressive failure, delamination, and shear failure. Compared with the tensile strength, a CFRP longitudinal laminate's compressive strength is significantly discounted due to carbon fiber buckling as the relatively much softer matrix provides little transversal support. These drawbacks limit the potential applications range of CFRPs. Therefore, many research efforts have been tied to address these weaknesses.

SAMPE Conference Proceedings. Charlotte, NC, May 20-23, 2019. Society for the Advancement of Material and Process Engineering – North America.

The use of nanofillers, e.g., carbon nanotubes, carbon nanofibers, carbon black, and graphene, have shown promising results to increase the material properties, e.g., mechanical, thermal and electrical, of CFRPs and glass fiber reinforced polymers (GFRPs) [1]. A recently developed process [2] allows one to manipulate long carbon nanofibers (CNFs), pre-dispersed in a polymer matrix, to thread through the array of carbon fibers in order to enhance the CFRP in the laminate's through-thickness direction (z-direction). With this new process, it is possible to manufacture CFRP prepreg containing zig-zag transverse-oriented CNFs (z-threaded CNFs) by flow-transferring a resin film containing electrical-field-aligned CNFs into a dry carbon fiber fabric. Figure 1 gives a basic representation of the ZT-CFRP with the CNFs threading through multiple carbon fiber arrays in the z-direction.

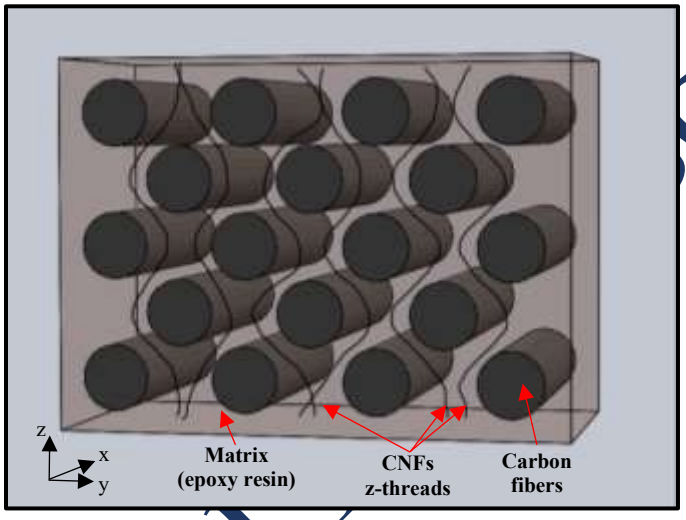

Figure 1. Illustration of ZT-CFRP structure.

Previous studies have shown that by using CNF z-threads, mechanical, thermal and electrical properties can be significantly improved even when using low CNF concentrations. Hsiao et al. [3] showed that additional reinforcement in the through-thickness direction, using 0.3wt% CNF z-threads (PS-CNF-PR24-XT), increases the mean for the Mode-I interlaminar fracture toughness (G_{IC}) of T300 carbon fiber plain weave (203 gsm) by ~29%. Meanwhile, the coefficient of variation reduces by ~12%. Scruggs et al. showed that the through-thickness DC electrical conductivity of z-threaded CNF laminates improves by 238% and 1508% with a CNF concentration of 0.1wt% (UD T700 carbon fiber) [4] and 1.0wt% (UD AS4 carbon fiber) [5], respectively, when compared to unmodified (control) CFRP laminates. Ranabhat and Hsiao [6] showed that CNF z-threads can even increase the through-thickness DC electrical conductivity of CFRP laminates up to 100 times compared to unmodified CFRP laminates using a radial flow-alignment process. In another study by Scruggs et al. [7], it was shown that the through-thickness thermal conductivity of AS4 CFRP laminates can be increased from 1.31 W/m-K to 9.85 W/m-K (+6531%) using 1.0wt% CNF z-threads. Also, due to the increase in thermal conductivity, the CFRP laminates modified with CNF z-threads therefore provided significantly better thermal infrared image transparency compared to the unmodified CFRP laminates. A previous study by the authors showed that the interlaminar shear strength (ILSS) of UD AS4 CFRPs improves by up to 35% using CNF z-threads [8, 9]. However, the contribution of z-threaded CNFs regarding longitudinal compressive strength has yet to be explored.

The hypothesis for this study was that long CNFs would thread through multiple arrays of carbon fibers in a zig-zag pattern along the z-direction of the laminate (as shown in Figure 1). This forms an interlocked multiscale fiber-reinforcement network, which provides stiffer transversal support against carbon fiber bucking thus enhances the compressive strength of the CNF z-threaded CFRP laminates. To find the answer for this hypothesis, an experimental investigation was conducted on the longitudinal compressive strength of CNF z-threaded CFRP laminates. The results were then compared to unmodified CFRP laminates and CFRP laminates modified with unaligned (randomly aligned) CNFs to separately understand the effects of CNFs as well as the z-threading strategy. The distinct morphology of the CNF z-threaded CFRP samples was investigated with a microscopy analysis to understand the roles of CNF z-threads during compression failure even further.

2.1 Literature Review

As previously mentioned, in the past two decades a large variety of research has been conducted to investigate different reinforcement methods using nanofillers. A literature review was conducted that summarizes previously performed studies utilizing a variety of nanofillers and manufacturing methods to better understand the possible effects of nanofillers on the compressive strength of fiber-reinforced composites prior to experimental testing of the ZT-CFRPs.

Anand et al. [10] used a Resin Film Infusion (RFI) process together with randomly aligned multi-walled carbon nanotubes (MWCNTs) dispersed in the epoxy matrix to improve the matrix-dominated properties of unidirectional E-glass reinforced with epoxy. Tests showed that the compressive strength could be improved by up to ~24% (from 620 MPa to 770 MPa) for MWCNF-modified E-glass composite laminates when compared to control (unmodified) E-glass laminates.

Zhou et al. [11] used 2wt% carbon nanofibers (CNFs) to modify the epoxy resin in order to improve the matrix-dominated properties of satin weaved carbon/epoxy composites using a vacuum-assisted resin infusion molding process (VARTIM). The compressive strength of the composite laminate reinforced with 2wt% CNFs improved by 19.8% (from 292 MPa to 350 MPa). The fiber volume fraction was determined as 56%. Environmental scanning electron microscopy (SEM) imaging showed that the improved mechanical properties for CNF-modified composites are likely due to some crack bridging and reduced crack opening, which results in crack turning for small cracks.

Iwahori et al. [12] dispersed carbon nanofibers (CNFs) in epoxy resin (EPIKOTE 827) with CNF concentrations of 5wt% and 10wt%. The modified resin mixture was used to impregnate a carbon fiber fabric (plain weave TORAYCA C6343 fabric). The laminate was cured using a hot press method. The concept was to determine if CNFs as a matrix modifier improve the interlaminar strength of CFRPs, and therefore increase the compressive strength. The compressive strength of the CFRP increased by up to 15% (from 446.8 MPa to 513.8 MPa) with a CNF concentration of 5wt%. However, no straight relationships have been established between CNF weight-content and compressive strength improvements. The reasons can be due to potentially non-homogeneous dispersion of CNFs into the epoxy matrix that creates CNF clusters, and the formation of void, which tend to produce stress concentration spots where crack initiation occurs at low-stress levels. They concluded that a higher weight content of CNF could increase the strength in tension, compression, and flexure. However, for this, the dispersion process has to be improved to reduce void within the laminates.

Liu et al. [13] used nanosilica, halloysite, and liquid rubber to reinforce the matrix of carbon fiber composites to evaluate the effect of the different filler material on the compressive and flexural properties of the composite. The samples with the different matrix reinforcement filler material and a control sample with no reinforcement filler material were manufactured using a vacuum assisted resin infusion molding (VARIM) process. The composite consisted of unidirectional T300 carbon fiber fabric (with a transverse polyester stitching), Bisphenol A diglycidyl ether (DGEBA) epoxy resin (Araldite-F from Huntsman), a hardener (piperidine from Sigma-Aldrich), and either of the nanofiller material. The different concentration of the different nanofillers within the epoxy varied between 2 – 20wt%. Compressive and flexural tests were performed to determine the effect of the nanofiller on the material properties of the composite. The study showed that flexural and compression properties can be significantly enhanced using nanosilica and halloysite, whereas using liquid rubber does not result in a significant increase or even in decreased properties. Halloysite had the highest compressive strength increase, 22.3% (from 367 MPa to 449 MPa) when compared to the unmodified CF composite. On the other hand, nanosilica, and liquid rubber had either an almost negligible increase in compressive strength of less than 6%, or even a decrease in compressive strength when compared to the unmodified CF composite.

Sharma and Lakkad [14] grew multi-walled carbon nanotubes (MWCNTs) directly on the surface of the carbon fibers using a thermal chemical vapor deposition (CVP) process at 700 °C in order to reinforce the interface between the carbon fibers and the polymer matrix of CFRP composites. The MWCNT-modified composite was then tested under compressive loading to determine the compressive properties. An unmodified CFRP composite that underwent the same thermal treatment as the MWCNT-modified composite was also manufactured using the same compression die molding manufacturing process as for the modified composite. The test results of the modified composite were then compared to the test results of the unmodified composite. To verify that the manufacturing process was successful, the authors used SEM images to evaluate the morphology of the carbon fibers and the composites. The test results show that the compressive strength for the MWCNT-modified carbon fiber composites was significantly enhanced by around 4% (from ~288 MPa to ~300 MPa) and around 67% (from ~73 MPa to ~122 MPa) in the longitudinal and transverse direction, respectively when compared to the unmodified CFRP.

The results found in the literature support the idea that dispersing stiff and strong nanoparticles in the matrix could help to improve the laminates' compressive strengths. Therefore, it would be interesting to understand the roles of the CNF z-threads during the compressive failure of CFRP laminates.

3. EXPERIMENTATION

For this study, the same materials and CFRP manufacturing procedures were used as published in previous publications by the authors [8, 9].

3.1 Materials

To determine the possible effects of the CNF z-threads, three different sample types were manufactured and subsequently compared to one another. The three different laminates are an unmodified CFRP (Control CFRP), a 1.0wt% (with respect to the weight of the matrix) randomly/unaligned CNF-modified CFRP (UA-CFRP), and a 1.0wt% CNF z-threaded CFRP (ZT-CFRP). Each sample type was produced from unidirectional (UD) HexTow^{TM} AS4 carbon fiber fabric (1.79 g/cm^3 fiber density, 3K tow-size, and 190 g/m^2 areal weight). The matrix was

EPON 862/Epikure-W resin purchased from Miller-Stephenson Chemical Co., Inc. The CNFs were PR-24-LD-HHT from Pyrograf Products, Inc and provided by Applied Science, Inc. The CNFs have an average diameter of 100 nm, and a length ranging from 50 µm to 100 µm [15]. Two surfactants were used, Disperbyk-191 and Disperbyk-192, provided by BYK USA, Inc, to assist the CNF dispersion within the resin mixture during sample manufacturing. [16, 17]

CNFs have an outstanding mechanical strength and moduli, with a Young's modulus of about 600 GPa and a tensile strength of around 7 GPa [18, 19]. For comparison, the Young's modulus and tensile strength of steel are around 200 GPa and 1 GPa to 2 GPa, respectively [20]. CNFs are weaker than carbon nanotubes (CNTs), whose Young's modulus and tensile strength can be 1400 GPa and 100 GPa, respectively [20]. However, due to their cup-stacked structure, CNFs provide better bonding with the polymer matrix and are typically longer and more affordable than CNTs. Therefore, the material is a favorable nanofiller to improve the mechanical properties of the polymer matrix considerably within fiber-reinforced composites.

3.2 CFRP Laminate Preparation

The manufacturing steps for the different CFRP types are shown in Figure 2. Further details about the individual manufacturing steps can be found in previous publications by the authors [8, 9]. The resin film containing z-aligned CNFs, which was used to manufacture the ZT-CFRP prepreg, was produced on a proprietary automated resin film production machine and collected on a continuous roll. The automated roll-to-roll ZT-CFRP prepreg production machine is currently under development.

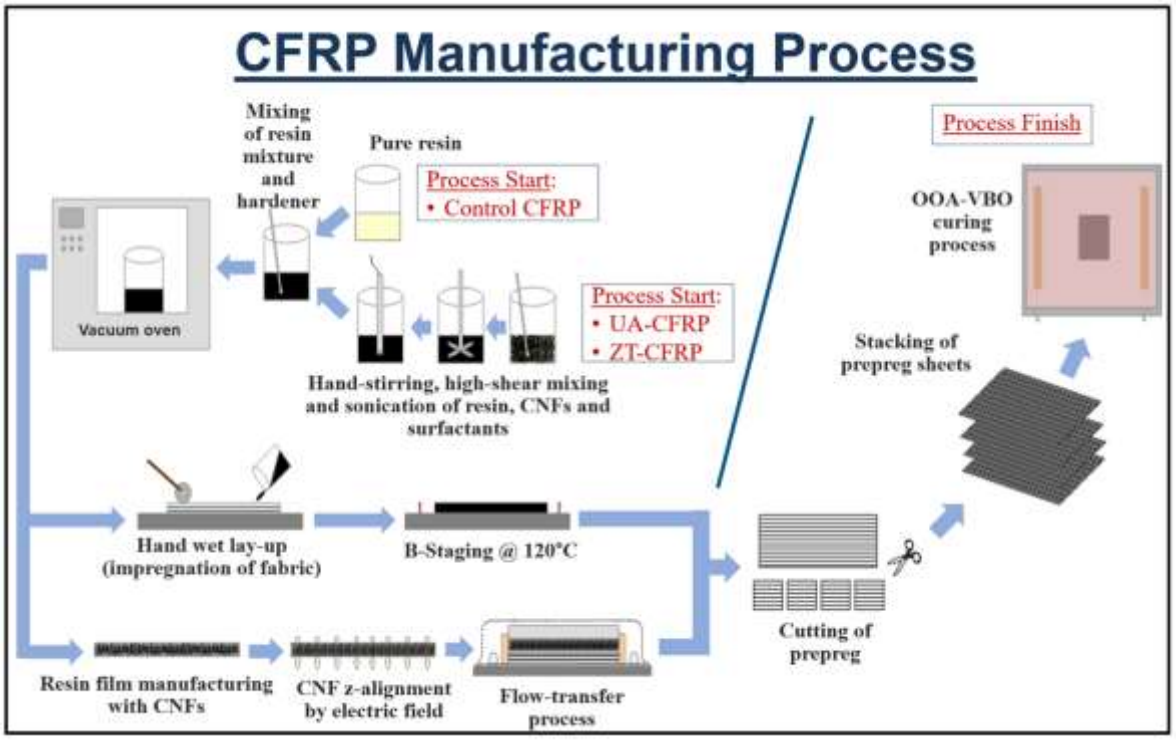

Figure 2. Step-by-step illustration of CFRP manufacturing process.

For each CFRP sample type, a 130 mm x 100 mm panel was manufactured from 10 prepreg plies. Five specimens each were then cut from the individual panel using a computer numerical control (CNC) router (CNC Shark Pro HD from Next Wave Automation). The specimen dimension conformed to dimensions suggested by the Recommended Method (SRM 1R-94) of the Suppliers of Advanced Composite Materials Association (SACMA) [21], with a specimen width of 15.0 mm, a specimen thickness of 1.02 mm, and a specimen length of 80.0 mm. A representation of the test specimen and its dimension is shown in Figure 3. Each specimen was tabbed with a Garolite G-10 epoxy-grade industrial laminate with fiberglass reinforcement purchased from McMaster-Carr. LOCTITE, a two-part heavy-duty epoxy resin system from Henkel with a maximum strength of 24 MPa was used to bond the tabs to the specimen. The gage length was 4.75 mm as suggested by SRM 1R-94 [21]. Before testing, the tabbed specimen cured for at least 24 hours at room temperature for full adhesive bonding of the tabs with the specimen.

3.3 Testing Procedures

Each unidirectional $[0]_{10}$ laminate sample type with each of its five specimens underwent the same testing procedure as suggested by SRM 1R-94 [21] to determine its compressive strength.

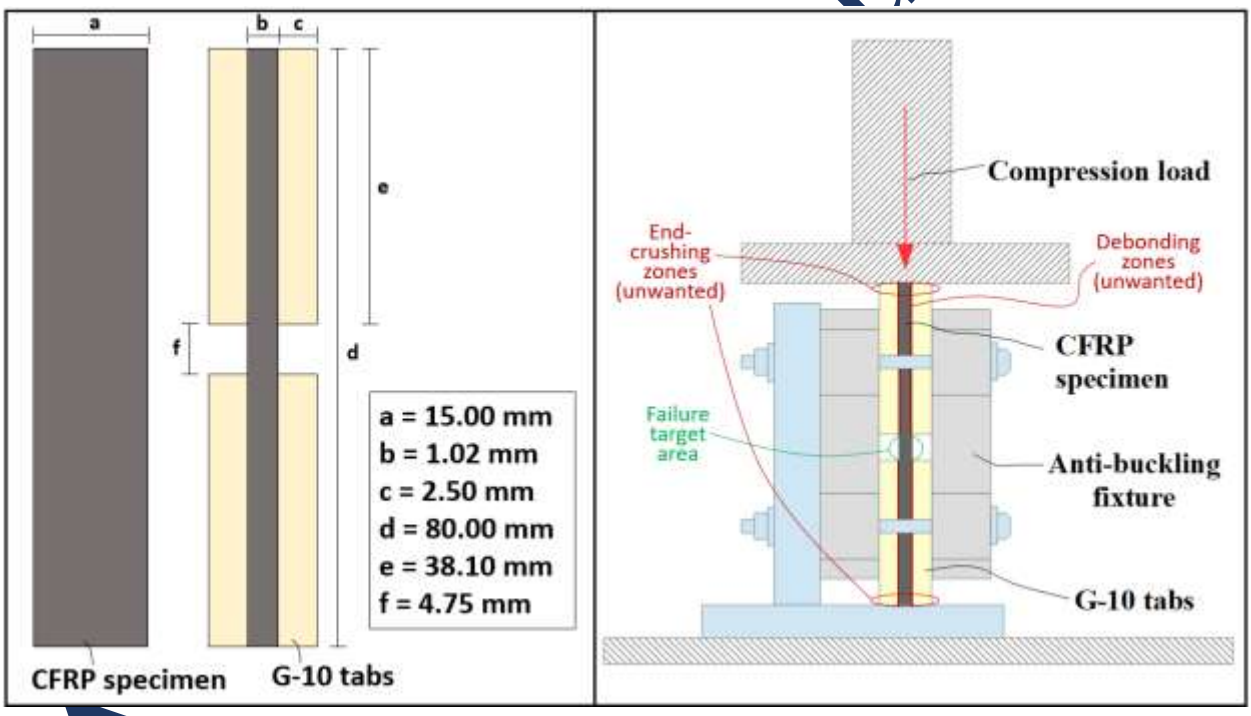

Figure 3. Test specimen dimension (left) and compression testing setup (right).

In addition, DC electrical conductivity measurements were taken of each specimen to ensure that the different manufacturing procedures have been successful. Previous studies have shown that the CNF z-threads significantly increase the DC electrical conductivity in the through-thickness direction compared to Control and UA-CFRPs [5]. Therefore, the z-directional DC electrical conductivity was used to verify the CNF alignment within the ZT-CFRP samples. A four-probe technique as described in previous studies [5] was chosen to avoid measurement errors that can occur due to contact resistance between the testing fixture and the CFRP samples. If the alignment

and the z-threading process were successful, the ZT-CFRP would show an electrical conductivity value similar to that reported before in studies by Scruggs et al. [5] due to proofed repeatability. Details about the through-thickness DC electrical conductivity measurement procedure can be found in a previous publication by the author [8].

The compression test was performed on a TINIUS OLSEN Super "L" Universal Testing Machine with a 53,379 N (12000 lbf) load cell. The crosshead loading rate was 1.0 mm/min. An anti-buckling fixture, as suggested by the standard [21], was used for accurate and consistent alignment of the test specimen. A representation of the testing setup is given in Figure 3.

3.4 Microscopic Morphology Study

For the Control CFRPs and ZT-CFRPs, the failure modes that occurred during testing were characterized and compared using a Nikon Eclipse LV150 optical microscope equipped with an extended depth of focus (EDF) module.

4. RESULTS

The carbon fiber volume fraction was determined for each sample type per ASTM D3171. Table 1 shows the average values of all five specimens for each sample type. The difference between the volume fractions is only minimal. The addition of 1wt% CNFs to the matrix contributed to 0.3 g/m^2 weight increase of the ZT-CFRP laminate compared to the unmodified CFRP laminate as determined by the composite rule of mixture.

Table 1. Carbon fiber volume fraction for various sample types.

Sample Type	Carbon Fiber Volume Fraction (%)
Control CFRP	57 ± 1
UA-CFRP	52 ± 1
ZT-CFRP	54 ± 1

The compression test was performed per modified version of ASTM D695 (i.e., SACMA SRM 1R-94) for five specimens of each sample type. Table 2 shows the average compressive strength results for all samples with an acceptable failure mode. Some of the specimens had end-crushing failure modes with tab debonding, which is not an acceptable failure mode, and therefore were excluded from the average calculation in Table 1. This unwanted failure mode can be due to 1. Test specimen conditions: Material brittleness may have been caused by curing mismanagement, and void areas could have been formed in the end edges of the testing specimens. 2. Test specimen tabbing method: Tabbing was performed by applying epoxy resin between the specimen and the tabs. The interfacial bonding of the adhesion may not be sufficient enough to endure the compression load. With these end failure modes, it was difficult to transfer the compression load throughout the specimen uniformly. Thus, the interested area along the gage length was not fully focused to investigate the actual compressive strength of these samples. For future mechanical tests, tabbing conditions need to be studied with stronger bonding. The testing data for each specimen, including the ones with an unacceptable failure mode, are given within the APPENDIX section in Table A-1,Table A-2, and Table A-3 for the Control CFRP laminate, 1.0wt% UA-CFRP laminate, and 1.0wt% ZT-CFRP laminate, respectively.

The unmodified CFRP laminate with a compressive strength of 673.85 MPa was used as a base value (control) to which all results of the two different CNF-modified CFRP laminates were compared. The compressive strength in this study is lower than some of the reported values of CFRPs manufactured from commercial prepreg and by autoclave curing. The reason for this can be due to different factors that occur during the manufacturing process, including the creation of fiber waviness and fiber misalignment from the use of distribution media during curing, as well as void creation during manufacturing, which can significantly reduce the compressive properties of CF composites [22, 23]. However, other researchers have shown similar compressive strength results compared to the results presented in this study when not using commercial prepreg. For example, Wei et al. [24] reported a compressive strength of ~640 MPa and ~670 MPa for unmodified UD T700 and T800 CFRP laminates with a 60% fiber volume fraction. Liu et al. [13] presented a longitudinal compressive strength of 367 MPa for UD T300 CFRP laminates with a fiber volume fraction of 65%, which were manufactured using a VARIM manufacturing process. The authors of the article provided a similar explanation about the influence on the compressive strength due to different factors that exist during manufacturing when not using commercial prepreg. Furthermore, Cho et al. [23] reported a compressive strength of 551 MPa for a UD carbon/epoxy composite laminate with a 55% fiber volume fraction produced by a vacuum assisted wet layup process. The authors reasoned that the lower compressive strength is due to fiber misalignment caused by crimps from the glass fiber yarns that hold together the dry UD carbon fiber fabric.

While the compressive strength values of this study are also lower than commercial prepreg cured by autoclave, in terms of a comparison study for the effect of CNFs and their alignment on the compressive properties of CFRPs, the reported results are still meaningful for understanding the compressive failure mechanisms and the relative compressive strength improvement comparison.

The ultimate strain was determined from the change of crosshead positions. For this, the crosshead position was divided by the original length of the specimen. For the 1.0wt% ZT-CFRP laminate, the compressive strength was increased by 14.83% (from 673.85 MPa to 773.76 MPa) when compared to the Control CFRP due to the CNF's interlaminar and intralaminar reinforcement. Whereas, the 1.0wt% UA-CFRP laminate experienced an 8.02% decrease (from 673.85 MPa to 619.84 MPa) in compressive strength compared to the Control CFRP laminate.

Table 2. Overview of testing results for compressive strength test specimen with an acceptable failure mode.

Sample Type	**Area (mm^2)**	**Ultimate Force (N)**	**Ultimate Strain (%)**	**Compressive Strength (MPa)**	**COV (%)**	**Relative Improvement of Compressive Strength w.r.t. Control CFRP (%)**
Control CFRP	15.34	10,337.7	1.18	673.85	9.41	N/A
UA-CFRP	15.27	9462.53	1.32	619.84	9.56	-8.02
ZT-CFRP	14.76	11401.22	1.19	773.76	9.33	+14.83

The increase in ZT-CFRP can be due to the CNF z-threads enveloping around the carbon fiber yarns as both interlaminar and intralaminar reinforcement, which could also provide additional stiffness support to decrease the internal instability of the carbon fibers in void or defect areas. Thus, the buckling failure occurs at the higher compression load. The decrease in compressive strength for the UA-CFRPs can be due to the CNFs being randomly dispersed in the matrix region, which could cause CNF clusters in the specimens [9]. The slightly lower fiber volume fraction could also have a small effect on the decreased compressive strength of the UA-CFRP laminates. This comparison study shows that CNF z-threads deliver positive effects to enhance the compressive strength of CFRP laminates.

Figure 4Figure 5, andFigure 6 show graphical results of the compressive strength versus ultimate strain (calculated from the crosshead position) for the Control CFRP, 1.0wt% UA-CFRP, and 1.0wt% ZT-CFRP samples. The specimen marked with an asterisk (*) experienced an unwanted end-crushing failure mode due to both tab-debonding as well as specimen end-crushing. If the failure occurred within the untabbed/gage section without tab debonding, the failure mode was acceptable and the test successful. Each CFRP sample type shows different failure trends. In Figure 4 and Figure 5, Control CFRP and UA-CFRP graphs show brittle failure as the compressive strength drastically drops after reaching the ultimate point for specimens with acceptable failure modes. This represents that there is no additional support after fiber breakage within the Control CFRP. The rounded peaks for the specimens with unacceptable failure modes are due to end-crushing and not fiber buckling as for the acceptable failure modes. In Figure 6, ZT-CFRP graphs show multiple failure stages as the CNF z-threads provide additional stiffness to ZT-CFRP specimens along with the interlaminar and intralaminar reinforcement for both acceptable and unacceptable failure modes. Further investigations have to be performed to understand better why for the ZT-CFRPs the peak of the graph is not rounded for specimens with unacceptable failure modes as it is the case for the Control and UA-CFRP samples. It is hypothesized that for acceptable failure modes, the first failure point of the graph represents fiber breakage, but unlikely the Control CFRP, CNFs within the ZT-CFRP continue to endure the load (graph going up) and provide the stiffness to stabilize the carbon fibers even after initial fiber buckling (or initial minor matrix cracks under compression). And finally, the second failure point of the graph represents that CNFs no longer endure the load and mechanically fail; thus the carbon fibers completely buckled and cause significant crack propagation.

A microscopic morphology study helped to better under the role of the CNFs during compression failure. Figure 7a) and b) show microscopic images of a cracked ZT-CFRP specimen after compression failure at 100× and 1000× magnifications, respectively. The microscopic images help to understand the ZT-CFRP structure better. At a 1000× magnification, it is possible to see the CNFs, which are sticking up and down in the through-thickness direction (i.e., z-direction) of the laminate. The length of the pulled-out CNFs is close to the carbon fiber diameter (~7 μm), and some of the CNFs are still connected, which proves the hypothesis of the CNFs interlocking the carbon fibers, and therefore reinforcing the CFRP laminate in the through-thickness direction.

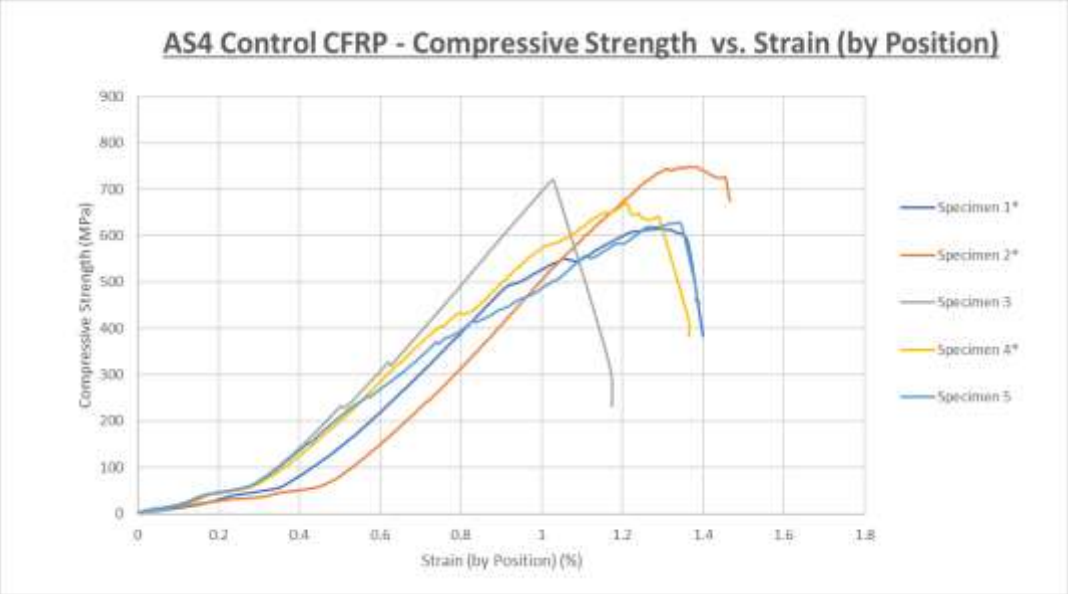

Figure 4. Compressive strength vs. crosshead position for Control CFRP laminate.

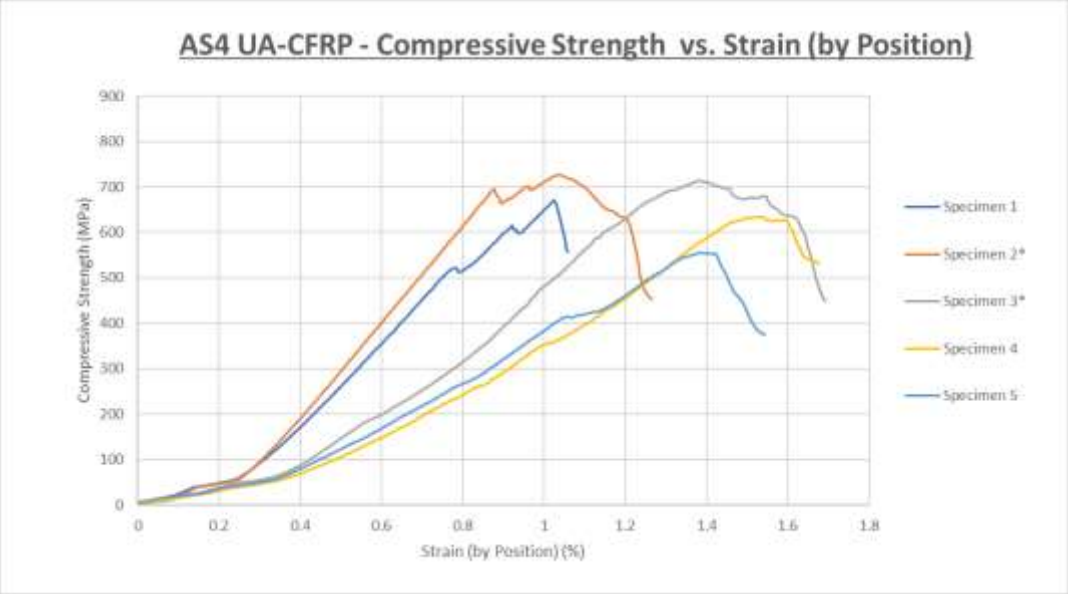

Figure 5. Compressive strength vs. crosshead position for 1.0wt% UA-CFRP laminate.

Figure 7c) shows an illustration of the ZT-CFRP laminate structure during crack propagation for further clarification. Here, Zone 1 has a matrix that is fully intact with no CNF pull-outs. Zone 2 and Zone 3 represent the crack-zones. The crack is propagating from Zone 3 towards Zone 1. Zone 2 has CNFs that are still interlocking the carbon fibers while the matrix has already cracked. In Zone 3, the matrix cracking has caused pulled-out CNFs. During compression loading, fiber buckling occurs, causing the matrix to crack slowly until ultimate failure of the specimen. The

z-threaded CNFs help to delay and stop crack growth and to distribute stress concentrations due to CNF/carbon fiber interlocking, which explains the multiple failure stages of the ZT-CFRPs as shown in Figure 6.

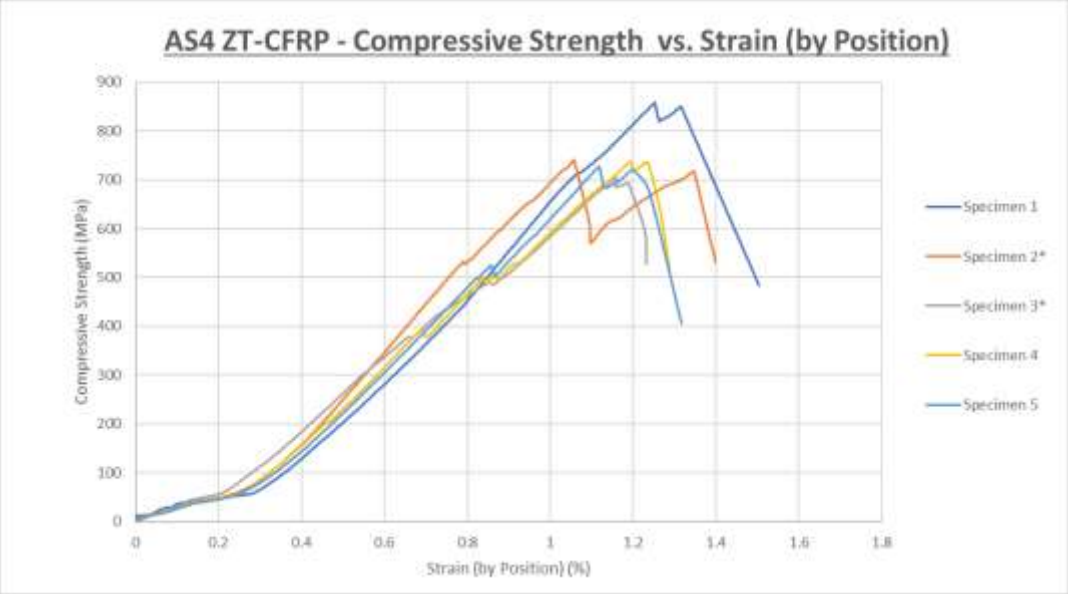

Figure 6. Compressive strength vs. crosshead position for 1.0wt% ZT-CFRP laminate.

5. CONCLUSIONS

The main reason for composites failure during compression is due to fiber buckling. In this study, it was hypothesized that carbon nanofiber z-threads incorporated into CFRP composites prevent fiber buckling in interlaminar and intralaminar regions and improve the longitudinal compressive strength of the CFRP laminates. To verify the hypothesis, longitudinal compression tests were conducted on Control CFRP, 1.0wt% CNF UA-CFRP and 1.0wt% CNF ZT-CFRP. The results showed that 1.0wt% CNF z-threaded CFRP laminates with a fiber volume fraction of 54% provide an improvement of ~15% (from 673.85 MPa to 773.76 MPa) over the Control CFRP laminates with a fiber volume fraction of 57%. Whereas, 1.0wt% UA-CFRP showed a decrement in compressive strength of ~8% (from 673.85 MP to 619.84 MPa) compared to the unmodified CFRP. The decline in compressive strength for the UA-CFRP is mainly due to agglomeration of CNFs within the laminates, which may create voids and therefore a weaker material structure. The multiple failures reported in ZT-CFRP are mainly due to the z- threaded CNFs, which provide additional stiffness along the interlaminar and intralaminar region of ZT-CFRP laminates due to CNF/carbon fiber interlocking. UA-CFRP laminate showed less brittle failure compared to Control CFRP laminate due to randomly oriented CNFs, which could provide additional reinforcement due to some of the CNFs being oriented in the optimal direction.

It was shown that CNF z-threads have a positive effect on the longitudinal compressive strength of CFRPs due to interlaminar and intralaminar reinforcement from CNF/carbon fiber interlocking, while only adding around 0.3 g/m^2 with a 1.0wt% CNF content. As mentioned throughout the report, some of the tested samples had unwanted failure modes due to tab debonding and end-crushing. Therefore, further tests have to be conducted to increase the sample size. In addition,

different fiber and resin types could be studied, as well as additional CNF concentration to find the optimal CNF/fiber/resin interaction in order to maximize the compressive strength of the CFRP. Furthermore, dynamic tests on ZT-CFRPs could also be the goal of future studies.

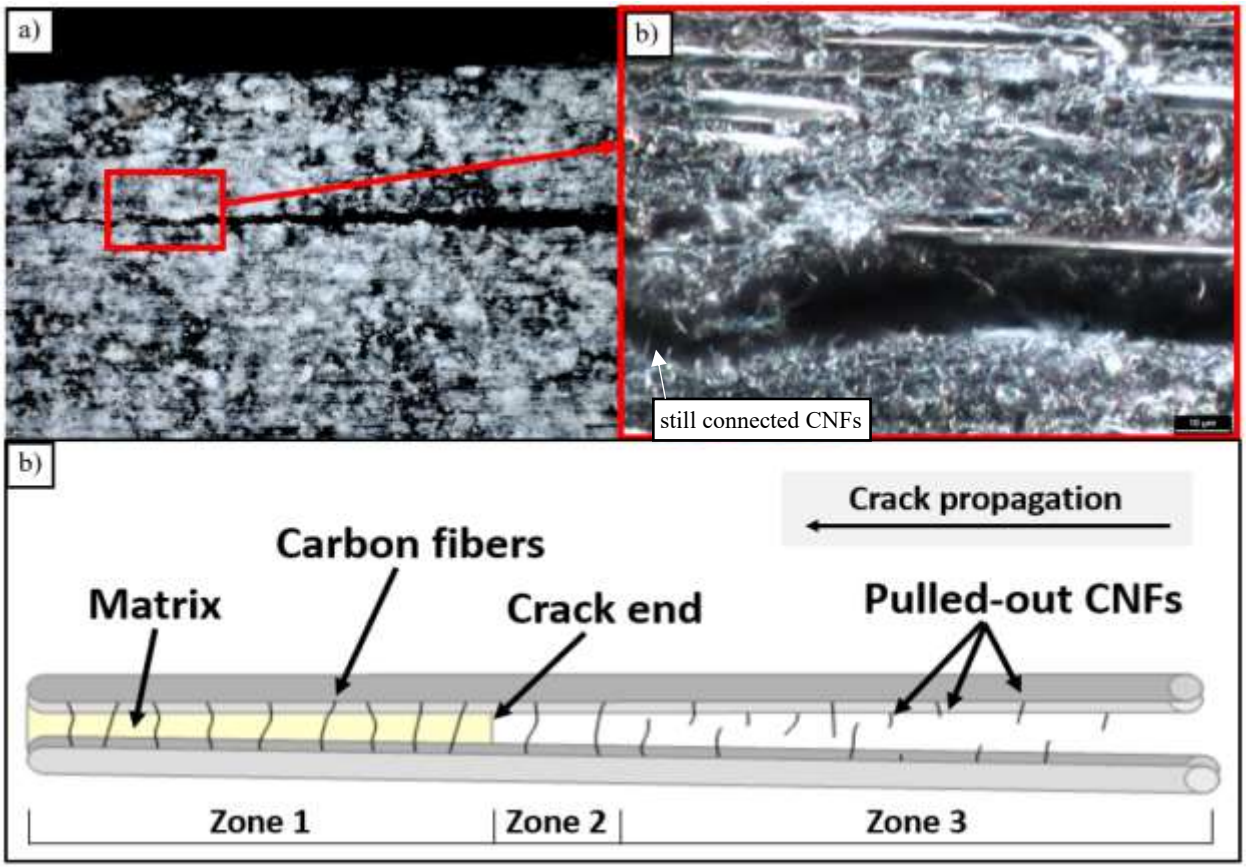

Figure 7. (a) 100× microscopic image, (b) 1000× microscopic image, and (c) illustration of crack in the ZT-CFRP laminate after compressive failure.

6. ACKNOWLEDGMENTS

The authors would like to acknowledge the financial support of the Alabama Department of Commerce (Alabama Innovation Fund, Award number: 150436), the College of Engineering's Systems Engineering Program Graduate Assistantship at the University of South Alabama, and the National Science Foundation (National Innovation Corps (I-Corps) Teams Program, Award number: 1748369). In addition, the authors are grateful for the carbon fiber materials provided by Hexcel Corporation, the carbon nanofiber materials provided by Applied Science, Inc, and the surfactants provided by BYK USA, Inc.

7. REFERENCES

1. Spitalsky, Z., Tasis, D., Papagelis, K., and Galiotis, C. "Carbon nanotube – polymer composites: Chemistry, processing, mechanical and electrical properties," *Progress in Polymer Science* 35(3) (2010): 357–401. DOI: 10.1016/j.progpolymsci.2009.09.003.

2. Hsiao, K.-T., and Hickman, G.J.S. “Novel Method for Manufacturing Nano-Structurally Aligned Multi-Scale Composites,” US 2016/0168342 A1, 2016.

3. Hsiao, K.T., Scruggs, A.M., Brewer, J.S., Hickman, G.J.S., McDonald, E.E., and Henderson, K. “Effect of carbon nanofiber z-threads on mode-I delamination toughness of carbon fiber reinforced plastic laminates,” *Composites Part A: Applied Science and Manufacturing* 91 (2016): 324–335. DOI: 10.1016/j.compositesa.2016.10.022.

4. Scruggs, A.M., Henderson, K., and Hsiao, K. “Characterization of Electrical Conductivity of a Carbon Fiber Reinforced Plastic Laminate Reinforced With Z-Aligned Carbon Nanofibers,” in *Proceedings of CAMX 2016 (The Composites and Advanced Materials Expo), Anaheim, CA, Sept. 26-29*, 2016, TP16-0137.

5. Scruggs, A.M. “Enhancement of Through-Thickness Electrical Conductivity Due to Carbon Nanofiber Z-Threads in Unidirectional Carbon Fiber Reinforced Plastic Laminates,” [M.S. Thesis]. Department of Mechanical Engineering, University of South Alabama, Mobile, Alabama, 2018.

6. Ranabhat, B., and Hsiao, K. “Improve the Through-Thickness Electrical Conductivity of Cfrp Improve the Through-Thickness Electrical Conductivity of CFRP Laminate Using Flow- Aligned Carbon Nanofiber Z-Threads,” in *Proceedings of SAMPE 2018 (Society for the Advancement of Material and Process Engineering), Long Beach, CA, May, 21-24*, 2018, SE18--1100.

7. Scruggs, A.M., Kirmse, S., and Hsiao, K.-T. “Enhancement of Through-Thickness Thermal Transport in Unidirectional Carbon Fiber Reinforced Plastic Laminates due to the Synergetic Role of Carbon Nanofiber Z-Threads,” *Journal of Nanomaterials* 2019 (2019): 1–13. DOI: 10.1155/2019/8928917.

8. Kirmse, S. “Interlaminar Shear Strength Enhancement of Unidirectional Carbon Fiber Reinforced Plastic Laminates Using a Carbon Nanofiber Z-Threading Technique,” [M.S. Thesis]. Department of Mechanical Engineering, University of South Alabama, Mobile, Alabama, 2018.

9. Kirmse, S., and Hsiao, K.-T. “Enhancing the Interlaminar Shear Strength of Unidirectional Carbon Fiber Reinforced Plastic (CFRP) Laminate Using a Nanofiber Z-Threading Strategy,” in *Proceedings of CAMX 2018 (The Composites and Advanced Materials Expo), Dallas, TX, Oct. 15-18*, 2018, TP18-0499.

10. Anand, A., Harshe, R., and Joshi, M. “Resin film infusion: Toward structural composites with nanofillers,” *Journal of Applied Polymer Science* 129(3) (2013): 1618–1624. DOI: 10.1002/app.38855.

11. Zhou, Y., Jeelani, S., and Lacy, T. “Experimental study on the mechanical behavior of carbon/epoxy composites with a carbon nanofiber-modified matrix,” *Journal of Composite Materials* 48(29) (2014): 3659–3672. DOI: 10.1177/0021998313512348.

12. Iwahori, Y., Ishiwata, S., Sumizawa, T., and Ishikawa, T. “Mechanical properties improvements in two-phase and three-phase composites using carbon nano-fiber dispersed resin,” *Composites Part A: Applied Science and Manufacturing* 36(10) (2005): 1430–1439. DOI: 10.1016/j.compositesa.2004.11.017.

13. Liu, F., Deng, S., and Zhang, J. “Mechanical Properties of Epoxy and Its Carbon Fiber Composites Modified by Nanoparticles,” *Journal of Nanomaterials* 2017 (2017): 1–9. DOI: 10.1155/2017/8146248.

14. Sharma, S.P., and Lakkad, S.C. “Compressive strength of carbon nanotubes grown on carbon fiber reinforced epoxy matrix multi-scale hybrid composites,” *Surface and Coatings Technology* 205(2) (2010): 350–355. DOI: 10.1016/j.surfcoat.2010.06.055.

15. “Pyrograf-III Carbon Nanofiber.” [Online]. Available: http://pyrografproducts.com/nanofiber.html#_PR-24-XT-HHT_Data_Sheet. [Accessed: 01-Oct-2018].

16. Hsiao, K.-T., and Gangireddy, S. “Investigation on the spring-in phenomenon of carbon nanofiber-glass fiber/polyester composites manufactured with vacuum assisted resin transfer molding,” *Composites Part A: Applied Science and Manufacturing* 39(5) (2008): 834–842. DOI: 10.1016/j.compositesa.2008.01.015.

17. Sadeghian, R., Gangireddy, S., Minaie, B., and Hsiao, K.-T. “Manufacturing carbon nanofibers toughened polyester/glass fiber composites using vacuum assisted resin transfer molding for enhancing the mode-I delamination resistance,” *Composites Part A: Applied Science and Manufacturing* 37(10) (2006): 1787–1795. DOI: 10.1016/j.compositesa.2005.09.010.

18. Lake, P.D. “Pyrograf III,” *Applied Sciences, Inc.*, 2012. [Online]. Available: http://apsci.com/?page_id=19. [Accessed: 01-Nov-2018].

19. Ozkan, T., Chen, Q., Naraghi, M., and Chasiotis, I. “Mechanical and interface properties of carbon nanofibers (CNFs) for polymer nanocomposites,” in *53rd International SAMPE symposium proceedings (Society for the Advancement of Material and Process Engineering), Memphis, TN, Sep. 8–11, 2008*, 2008.

20. Qin, Q.H. “Introduction to the composite and its toughening mechanisms,” in *Toughening Mechanisms in Composite Materials*, Q. Qin and J. Ye, Eds. Australian National University, Acton, ACT, Australia: Woodhead Publishing Series in Composites Science and Engineering, 2015, 1–32. DOI: 10.1016/B978-1-78242-279-2.00001-9.

21. “SACMA Recommended Test Method for Compressive Properties of Oriented Fiber-Resin Composites (SRM 1R-94),” Supplier of Advanced Composite Materials Association (SACMA).

22. Hsiao, H.M., and Daniel, I.M. “Effect of fiber waviness on stiffness and strength reduction of unidirectional composites under compressive loading,” *Composites Science and Technology* 56(5) (1996): 581–593. DOI: 10.1016/0266-3538(96)00045-0.

23. Cho, J., Chen, J.Y., and Daniel, I.M. “Mechanical enhancement of carbon fiber/epoxy composites by graphite nanoplatelet reinforcement,” *Scripta Materialia* 56(8) (2007): 685–688. DOI: 10.1016/j.scriptamat.2006.12.038.

24. Wei, W., Rongjin, H., Chuanjun, H., Zhao, Y., Li, S., and Laifeng, L. “Cryogenic performances of T700 and T800 carbon fibre-epoxy laminates,” in *IOP Conference Series: Materials Science and Engineering*, 2015, 102(012016). DOI: 10.1088/1757-899X/102/1/012016.

8. APPENDIX

Table A-1. Compressive strength data for Control CFRP laminate.

AS4 Control CFRP - Compressive Strength (Test Results)									
Specimen	**Specimen Length (mm)**	**Specimen Thickness (mm)**	**Specimen Width (mm)**	**Area (mm^2)**	**Ultimate Force (N)**	**Ultimate Strain (%)**	**Failure Mode**	**Compresive Strength (MPa)**	
AS4 Control 1	80.01	1.075	15.09	16.22	9957.62	1.29	Debonding & End-Crushing	613.95	**Compressive Strength Improvement w.r.t. Control (%)**
AS4 Control 2	79.96	1.028	15.05	15.46	11590.38	1.37	Debonding & End-Crushing	749.51	
AS4 Control 3	80.01	1.028	14.98	15.39	11063.69	1.03	Compressive Failure	718.68	
AS4 Control 4	79.99	1.038	14.97	15.53	10424.15	1.21	Debonding & End-Crushing	671.06	
AS4 Control 5	80.00	1.018	15.02	15.28	9611.75	1.34	Compressive Failure	629.03	
Average	79.99	1.04	15.02	15.58	10529.52	1.25	-	676.44	N/A
STDEV	0.02	0.02	0.05	0.37	804.87	0.14	-	57.68	
Maximum	80.01	1.08	15.09	16.22	11590.38	1.37	-	749.51	
Minimum	79.96	1.02	14.97	15.28	9611.75	1.03	-	613.95	
COV (%)	0.03	2.16	0.32	2.38	7.64		-	8.53	

Table A-2. Compressive strength data for 1.0wt% UA-CFRP laminate.

AS4 UA-CFRP - Compressive Strength (Test Results)									
Specimen	**Specimen Length (mm)**	**Specimen Thickness (mm)**	**Specimen Width (mm)**	**Area (mm^2)**	**Ultimate Force (N)**	**Ultimate Strain (%)**	**Failure Mode**	**Compresive Strength (MPa)**	
AS4 UA 1	80.00	1.025	15.03	15.41	10331.00	1.02	Compressive Failure	670.59	**Compressive Strength Improvement w.r.t. Control (%)**
AS4 UA 2	80.01	1.030	14.95	15.40	11177.19	1.04	Debonding & End-Crushing	725.86	
AS4 UA 3	79.99	1.010	14.95	15.10	10769.95	1.38	Debonding & End-Crushing	713.15	
AS4 UA 4	80.00	1.003	14.88	14.91	9459.60	1.54	Compressive Failure	634.25	
AS4 UA 5	79.99	1.035	14.98	15.50	8596.99	1.39	Compressive Failure	554.68	
Average	80.00	1.02	14.96	15.26	10066.95	1.27	-	659.71	-2.47
STDEV	0.01	0.01	0.05	0.25	1039.98	0.23	-	68.98	
Maximum	80.01	1.04	15.03	15.50	11177.19	1.54	-	725.86	
Minimum	79.99	1.00	14.88	14.91	8596.99	1.02	-	554.68	
COV (%)	0.01	1.35	0.31	1.61	10.33		-	10.46	

Table A-3. Compressive strength data for 1.0wt% ZT-CFRP laminate.

AS4 ZT-CFRP - Compressive Strength (Test Results)									
Specimen	**Specimen Length (mm)**	**Specimen Thickness (mm)**	**Specimen Width (mm)**	**Area (mm^2)**	**Ultimate Force (N)**	**Ultimate Strain (%)**	**Failure Mode**	**Compresive Strength (MPa)**	
AS4 ZT 1	79.99	0.955	14.94	14.27	12223.80	1.25	Compressive Failure	856.89	**Compressive Strength Improvement w.r.t. Control (%)**
AS4 ZT 2	80.02	1.013	14.91	15.09	11174.35	1.06	Debonding & End-Crushing	740.45	
AS4 ZT 3	80.02	1.010	14.93	15.08	10608.48	1.16	Debonding & End-Crushing	703.40	
AS4 ZT 4	79.99	1.018	14.86	15.12	11152.07	1.19	Compressive Failure	737.69	
AS4 ZT 5	80.00	0.993	15.01	14.90	10827.81	1.12	Compressive Failure	726.70	
Average	80.00	1.00	14.93	14.89	11197.30	1.16	-	753.03	11.32
STDEV	0.02	0.03	0.06	0.36	620.38	0.07	-	59.87	
Maximum	80.02	1.02	15.01	15.12	12223.80	1.25	-	856.89	
Minimum	79.99	0.96	14.86	14.27	10608.48	1.06	-	703.40	
COV (%)	0.02	2.56	0.38	2.42	5.54		-	7.95	